

DOI: 10.51981/2588-0039.2024.47.005

REFERENCE RESPONSES OF REGIONAL ELECTRON CONTENT TO STRONG GEOMAGNETIC EVENTS

K.G. Ratovsky¹, M.V. Klimenko², A.M. Vesnin¹, K.V. Beluchenko¹

¹*Institute of Solar-Terrestrial Physics SB RAS, Irkutsk, Russia*

²*West Department of Pushkov Institute of Terrestrial Magnetism, Ionosphere and Radio Wave Propagation RAS, Kaliningrad, Russia*

Abstract. The paper presents an analysis of reference responses of regional electron content to strong geomagnetic events identified by the AE-index. As an ionospheric characteristic, we used the regional electron content (REC), which is the average total electron content (TEC) for five latitude zones in the corrected geomagnetic coordinate system: the mid-latitude zones in both hemispheres, the high-latitude zones in both hemispheres, and the equatorial zone. The relative (percentage) deviation of observed values from the 27-day running average REC was used to calculate disturbances of REC (Δ REC). The reference response was calculated by averaging Δ REC using the superimposed epoch method with key moments corresponding to the AE maximum for the winter, spring, summer and autumn storms. The paper discusses storm-time behavior, seasonal dependence and interhemispheric asymmetry of the REC responses to strong geomagnetic events.

Introduction

Solar, geomagnetic and meteorological activities contribute to the overall variability of the ionosphere. Statistical analysis of ionospheric responses to geomagnetic storms [Ratovsky *et al.*, 2018] showed that even in the case of isolated storms occurring in the same seasons and at approximately the same time of day, ionospheric responses can differ significantly from each other. Such differences can be caused by ionospheric disturbances of meteorological origin that have sources in the lower atmosphere, as well as the uniqueness of the scenario of each geomagnetic storm. Within the framework of the statistical approach to the study of ionospheric responses to geomagnetic events, we expect that the average ionospheric response will be mainly due to the effects of the geomagnetic event itself, while the influence of solar activity and processes in the lower atmosphere will be reduced due to averaging.

Data analysis method

In this paper, we used geomagnetic activity indices and global ionospheric total electron content (TEC) maps for 1999-2018. The year 1999 was chosen because this year is the first year of complete global TEC maps. The year 2018 was chosen because the AE-indices in open databases are available only for 2018. In the further analysis, the hourly average AE was used. The method for identifying geomagnetic events based on the AE index is described in detail in [Ratovsky *et al.*, 2024]. The criterion for a strong geomagnetic event identified by the AE-index was the fulfillment of two conditions: (1) AE(t_0) is the highest AE value over the time interval $t_0 \pm 12$ hours; and (2) AE(t_0) \geq 1280 nT, where t_0 is the time corresponding to the AE maximum. Using the above criteria, 103 strong geomagnetic events were identified. These events are geomagnetic storms (usually strong or moderate) according to the Dst-criterion, with the exception of three winter, two summer and one autumn event. Hereinafter, the strong geomagnetic events identified by the AE-index are designated as the strong AE-storms. To study the seasonal dependence of ionospheric responses, the strong AE storms were divided into seasons centered relative to the solstices and equinoxes in the Northern hemisphere: winter (Nov 07 – Feb 05, 21 AE-storms); spring (Feb 06 – May 07, 21 AE-storms); summer (May 08 – Aug 07, 35 AE-storms) and autumn (Aug 08 – Nov 06, 26 AE-storms).

The regional electron contents (REC), which are weighted average TEC values for the selected latitude and longitude region, were used as ionospheric characteristics. The TEC values were obtained from the global ionospheric maps of the CODE laboratory [Schaer *et al.*, 1998]. Five latitudinal zones in the corrected geomagnetic coordinate system were selected for calculating REC: mid-latitude zones in both hemispheres (30-60°), high-latitude zones in both hemispheres (60-90°), and the equatorial zone ($\pm 30^\circ$). The relative (percentage) deviations of the observed values from the 27-day moving average of REC were used to calculate REC disturbances (Δ REC). Using the superimposed epoch method with key moments corresponding to the AE index maximum, the averaged Δ REC behavior as the function of storm-time relative to the AE maximum ($\langle \Delta$ REC \rangle , reference ionospheric response) was calculated for the strong winter, spring, summer and autumn AE storms.

Analysis and interpretation of reference ionospheric responses to strong AE-storms

Figure 1 shows the AE-index averaged behavior for 4 seasons and the reference ionospheric responses for 4 seasons and 5 latitude zones. In all cases, the season is understood as winter, spring, autumn, and summer in the Northern hemisphere.

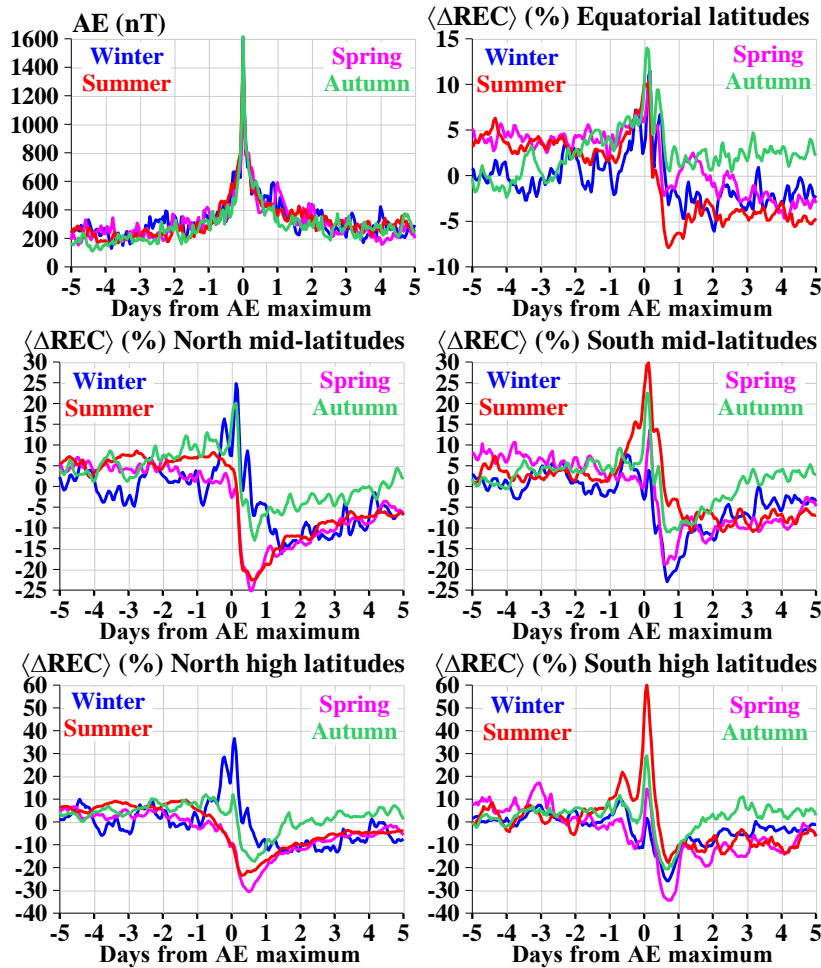


Figure 1. Averaged AE-index behaviors (top left) and reference ionospheric responses for equatorial zone (top right), mid-latitude zone (middle, Northern hemisphere on the left – Southern hemisphere on the right) and high-latitude zone (bottom, Northern hemisphere on the left – Southern hemisphere on the right). Winter is shown in blue, spring in magenta, summer in red and autumn in green.

As seen from Figure 1, the averaged AE-index behaviors for different seasons differ insignificantly, which allows us to ignore the seasonal differences in AE storms when interpreting ionospheric responses. The response behaviors and after the AE maximum shows that they can be divided into three types: A-type, N-type, and V-type. A-type responses have a well-defined maximum and a weakly-defined minimum. V-type responses have a well-defined minimum and a weakly-defined maximum. N-type response is characterized by both a well-defined maximum and a well-defined minimum. Table 1 presents the maximum and minimum values of the AE index and the $\langle \Delta \text{REC} \rangle$ reference responses, as well as the times of their maxima and minima relative to the AE maximum. As shows Table 1, A-type responses are seen in the Equatorial zone and only for local winters in the mid- and high-latitude zones, V-type responses are seen only for local summers and spring in the mid- and high-latitude zones, N-type responses are seen in all zones, the autumn responses are always of this type except for the equatorial zone. All well-defined maxima are in the narrow interval: 1-4 hours after the AE maximum. Mainly, the well-defined minima are in the narrow interval: 14-17 hours after the AE maximum, the exceptions are mid-latitude winter (35 hours) and high-latitude summer (7 hours) in the Northern hemisphere.

According to the thermospheric storm concept [Mayr et al., 1978; Field and Rishbeth, 1997; Ratovsky et al., 2018], the following seasonal dependence of electron density (N_e) disturbances is expected in the mid-latitude zone: the most negative disturbances in local summer and the most positive disturbances in local winter with intermediate disturbances at equinoxes. As seen from Figure 1 and Table 1, the seasonal structure of the mid-latitude response in the Southern hemisphere is fully consistent with the thermospheric storm concept, whereas in the Northern hemisphere

the spring response is as negative as the summer one. Note that in the Southern hemisphere, the spring response is much more negative than the autumn response. The reason for such negative ionospheric storms in the spring is currently unclear. According to the thermospheric storm concept [Mayr *et al.*, 1978; Field and Rishbeth, 1997; Ratovsky *et al.*, 2018], high-latitude ionospheric responses should be negative, but Figure 1 and Table 1 show huge positive responses in the high-latitude zone.

Table 1. Maximum (Max) and minimum (Min) values of AE-indices and $\langle\Delta\text{REC}\rangle$ reference responses. The sign after season indicates the response type, the Hours show the times of the maximum and maximum relative to AE-index maximum. Weakly-defined extremes are marked in italics.

AE-index (nT)					$\langle\Delta\text{REC}\rangle$ (%), Equatorial zone				
Season	Max	Hours	Min	Hours	Season	Max	Hours	Min	Hours
Winter(A)	1593	0	<i>129</i>	<i>-92</i>	Winter(A)	11.5	4	<i>-6.1</i>	<i>49</i>
Spring(A)	1483	0	<i>153</i>	<i>84</i>	Spring(A)	11	4	<i>-4.8</i>	<i>100</i>
Autumn(A)	1615	0	<i>109</i>	<i>-84</i>	Autumn(A)	14	2	<i>-2.4</i>	<i>-96</i>
Summer(A)	1462	0	<i>163</i>	<i>62</i>	Summer(N)	10.2	3	<i>-7.9</i>	<i>17</i>
$\langle\Delta\text{REC}\rangle$ (%), Mid-latitude zone of Northern hemisphere					$\langle\Delta\text{REC}\rangle$ (%), Mid-latitude zone of Southern hemisphere				
Season	Max	Hours	Min	Hours	Season	Max	Hours	Min	Hours
Winter(N)	24.8	3	<i>-16.2</i>	<i>35</i>	Winter(V)	7.7	<i>-12</i>	<i>-23</i>	<i>16</i>
Spring(V)	<i>7.4</i>	<i>-47</i>	<i>-25.2</i>	<i>14</i>	Spring(N)	13.7	4	<i>-18.8</i>	<i>14</i>
Autumn(N)	20.1	3	<i>-13</i>	<i>16</i>	Autumn(N)	22.5	2	<i>-11</i>	<i>16</i>
Summer(V)	<i>8.6</i>	<i>-66</i>	<i>-22.6</i>	<i>14</i>	Summer(A)	29.8	3	<i>-11</i>	<i>33</i>
$\langle\Delta\text{REC}\rangle$ (%), High-latitude zone of Northern hemisphere					$\langle\Delta\text{REC}\rangle$ (%), High-latitude of Southern hemisphere				
Season	Max	Hours	Min	Hours	Season	Max	Hours	Min	Hours
Winter(A)	36.6	2	<i>-13.2</i>	<i>74</i>	Winter(V)	9.8	<i>-16</i>	<i>-25.9</i>	<i>16</i>
Spring(V)	<i>6.7</i>	<i>-109</i>	<i>-30.6</i>	<i>12</i>	Spring(V)	<i>17.1</i>	<i>-73</i>	<i>-34.4</i>	<i>17</i>
Autumn(N)	12	1	<i>-23.5</i>	<i>16</i>	Autumn(N)	28.9	2	<i>-20.6</i>	<i>15</i>
Summer(V)	<i>9.6</i>	<i>-32</i>	<i>-17.4</i>	<i>7</i>	Summer(N)	60	2	<i>-17.9</i>	<i>17</i>

The high-latitude responses show the need to take into account the mechanisms for the formation of positive disturbances, which are absent in the thermospheric storm concept. Changes in Ne within the thermospheric storm concept primarily relate to heights near the ionospheric F2 layer maximum. As the height increases, the influence of changes in the neutral thermospheric composition weakens, and the influence of the electron temperature increases. An increase in the electron temperature leads to an increase in the scale height of the topside ionosphere, which can lead to a positive disturbance of TEC (which is proportional to the scale height of the topside ionosphere) under a negative disturbance of Ne near the F2 layer maximum. This version is confirmed by the results of [Astafyeva *et al.*, 2015; Klimenko *et al.*, 2017; 2018], where they demonstrated that the responses of the bottomside and topside ionosphere to a geomagnetic storm can have opposite signs. The seasonal structure of responses in the high-latitude zones of the Southern and Northern hemisphere can be explained as follows. In winter conditions, the background scale height of the topside ionosphere is minimal relative to other seasons, and, accordingly, the effect of increasing scale height s leads to the largest positive TEC. In summer conditions, the background scale height of the topside ionosphere is maximal, and, accordingly, the effect of increasing scale height is minimal.

The differences between the Northern and Southern hemispheres are manifested primarily in the much larger positive response in the high-latitude zone of the Southern hemisphere. The differences in the peak of the positive response are 60 and 37% for local winter and 29 and 12% for autumn. In the mid-latitude zone, the differences are somewhat smaller: 30 and 25% for local winter and 23 and 20% for autumn. Comparing the most negative responses, we note that the mid-latitude response is more negative in the Northern hemisphere (due to the strong negative spring response), while the high-latitude response is more negative in the Southern hemisphere (due to the strong negative spring response again). A similar (but not completely coinciding) interhemispheric asymmetry was reported by

Titheridge and Buonsanto [1988]. Titheridge and Buonsanto [1988] attributed the interhemispheric asymmetry in the ionospheric response to interhemispheric difference in the background neutral composition of the thermosphere. This explanation does not explain why the interhemispheric asymmetry is more pronounced at high latitudes. An alternative explanation is that the electron and thermospheric density responses are more sensitive to geomagnetic storms in the Southern hemisphere than in the Northern hemisphere [Ercha et al., 2012].

Conclusion

A statistical study of regional electron content responses to strong AE storms at high, mid, and equatorial latitudes, obtained by the epoch superposition method using the AE index, yielded the following main results.

The regional electron content responses can be divided into three types. A-type responses have a well-defined maximum and a weakly-defined minimum. V-type responses have a well-defined minimum and a weakly-defined maximum. N-type response is characterized by both a well-defined maximum and a well-defined minimum. All well-defined maxima are in the narrow interval: 1-4 hours after the AE maximum. Mainly, the well-defined minima are in the narrow interval: 14-17 hours after the AE maximum, the exceptions are mid-latitude winter (35 hours) and high-latitude summer (7 hours) in the Northern hemisphere.

The seasonal structure of the responses fully corresponds to the concept of a thermospheric storm only in the mid-latitude zone of the Southern hemisphere.

An increase in electron temperature, leading to an increase in the scale height of the topside ionosphere and in corresponding increase in the total electron content, is proposed as the cause of positive responses in the high-latitude zone. The greatest effect is achieved in winter conditions, when the background scale height of the topside ionosphere is minimal relative to other seasons.

The differences between the Northern and Southern hemispheres are manifested primarily in the much larger positive response in the high-latitude zone of the Southern hemisphere. In the mid-latitude zone, the differences are somewhat smaller. The peak negative mid-latitude response is more negative in the Northern hemisphere (due to the strong negative spring response), while the peak negative high-latitude response is more negative in the Southern hemisphere (due to the strong negative spring response again).

Acknowledgments

The study was supported by the Russian Science Foundation grant No. 23-27-00213. OMNI data were obtained via the GSFC/SPDFOMNI-Web interface at <https://omniweb.gsfc.nasa.gov>. The authors are grateful to the CODE laboratory for global ionospheric maps available at <ftp://ftp.unibe.ch/aiub/CODE/>. Primary series of regional electron content were obtained using the SIMuRG system, website <https://simurg.iszf.irk.ru/>.

References

- Astafyeva, E., Zakharenkova, I., Förster, M.: Ionospheric response to the 2015 St. Patrick's Day storm: A global multi-instrument overview, *J. Geophys. Res. Space Phys.*, 120, 9023–9037, <https://doi.org/10.1002/2015JA021629>, 2015.
- Ercha, A., Ridley, A.J., Zhang, D., Xiao, Z.: Analyzing the hemispheric asymmetry in the thermospheric density response to geomagnetic storms, *J. Geophys. Res.*, 117, A08317, <https://doi.org/10.1029/2011JA017259>, 2012.
- Field, P.R., Rishbeth, H.: The response of the ionospheric F2-layer to geomagnetic activity: an analysis of worldwide data. *J. Atmos. Solar-Terr. Phys.*, 59, 163–180, [https://doi.org/10.1016/S1364-6826\(96\)00085-5](https://doi.org/10.1016/S1364-6826(96)00085-5), 1997.
- Klimenko, M.V., Klimenko, V.V., Zakharenkova, I.E., Ratovsky, K.G., Korenkova, N.A., Yasyukevich, Y.V., Mylnikova, A.A., Cherniak, I.V.: Similarity and differences in morphology and mechanisms of the foF2 and TEC disturbances during the geomagnetic storms on 26–30 September 2011, *Ann. Geophys.*, 35, 923–938, <https://doi.org/10.5194/angeo-35-923-2017>, 2017.
- Klimenko, M.V., Klimenko, V.V., Despirak, I.V., Zakharenkova, I.E., Kozelov, B.V., Cherniakov, S.M., Andreeva, E.S., Tereshchenko, E.D., Vesnin, A.M., Korenkova, N.A., Gomonov, A.D., Vasiliev, E.B., Ratovsky K.G.: Disturbances of the thermosphere-ionosphere-plasmasphere system and auroral electrojet at 30°E longitude during the St. Patrick's Day geomagnetic storm on 17–23 March 2015, *J. Atmos. Solar-Terr. Phys.*, 180, 78–92, <https://doi.org/10.1016/j.jastp.2017.12.017>, 2018.
- Mayr, H.G., Harris, I., Spencer, N.W.: Some properties of upper atmosphere dynamics, *Rev. Geophys.*, 16, 539–565, <https://doi.org/10.1029/RG016i004p00539>, 1978.
- Ratovsky, K.G., Klimenko, M.V., Klimenko, V.V., Chirik, N.V., Korenkova, N.A., Kotova, D.S.: After-effects of geomagnetic storms: statistical analysis and theoretical explanation, *Solar Terrestrial Physics*, 4, 26–32, <https://doi.org/10.12737/stp-44201804>, 2018.
- Ratovsky, K.G., Klimenko, M.V., Vesnin, A.M., Belyuchenko, K.V., Yasyukevich, Y.V.: Comparative analysis of geomagnetic events identified according to different indices, *Bull. Russ. Acad. Sci. Phys.*, 88, 296–302, <https://doi.org/10.1134/S1062873823705433>, 2024.
- Titheridge, J.E., Buonsanto, M.J.: A Comparison of Northern and Southern Hemisphere TEC storm behaviour, *J. Atmospheric Terrest. Phys.*, 50, 763–780, [https://doi.org/10.1016/0021-9169\(88\)90100-6](https://doi.org/10.1016/0021-9169(88)90100-6), 1988.